jet INTL JOURNAL OF ELECTRONICS AND TELECOMMUNICATIONS, 2012, VOL. 58, NO. 4, PP. 425–431
Manuscript received November 8, 2012; revised Decemer, 2012. DOI: 10.2478/v10177-012-0058-7

Automated Characterization of Atheromatous Plaque in Intravascular Ultrasound Images Using Neuro Fuzzy Classifier

D. Selvathi, N. Emimal, and Henry Selvaraj

***Abstract*—The medical imaging field has grown significantly in recent years and demands high accuracy since it deals with human life. The idea is to reduce human error as much as possible by assisting physicians and radiologists with some automatic techniques. The use of artificial intelligent techniques has shown great potential in this field. Hence, in this paper the neuro fuzzy classifier is applied for the automated characterization of atheromatous plaque to identify the fibrotic, lipidic and calcified tissues in Intravascular Ultrasound images (IVUS) which is designed using sixteen inputs, corresponds to sixteen pixels of instantaneous scanning matrix, one output that tells whether the pixel under consideration is Fibrotic, Lipidic, Calcified or Normal pixel. The classification performance was evaluated in terms of sensitivity, specificity and accuracy and the results confirmed that the proposed system has potential in detecting the respective plaque with the average accuracy of 98.9%.**

***Keywords*—Intravascular ultrasound, atheromatous plaque, pixel intensity, neuro fuzzy classifier.**

I. Introduction

CARDIOVASCULAR diseases caused by the formation of plaque in coronary artery are the leading cause of mortality in the developed countries and it is estimated that, by 2030 there will be almost 23.6 million deaths [1]. However, the manual identification of plaque is not straightforward since it is susceptible to prolonged and human error intrusion process. Hence the main goal is automated characterization of plaque at the premier stage of development in patients who have a high risk of ischemic events.

Several approaches have been used for the characterization of atheromatous plaque. Some of them are semi-automatic and some of them are fully automatic. Semi-automatic methods require human intervention before it is given to the computer for processing. Amin Katouzian et al [2] described the realistic challenges in atherosclerotic plaque characterization. They explored the best reliable way to extract the most informative features and the classification algorithm which is most appropriate for this problem. Efthyvoulos C. Kyriacou et al [3] provides an overview of the several texture-feature extractions and classification methods and a summary of emerging trends and future directions in 3-D imaging methods and plaque-motion analysis. L.S Athanasiou et al [4] proposed a plaque characterization technique using two geometrical features such as the first geometrical feature describes the relative position of the pixel from the outer border (media-adventitia) of the ROI and the second geometrical feature describes the relative position of a pixel from the outer border (media-adventitia) and from the inner border (lumen) of the ROI. An overall classification accuracy of 84.45% is reported and is not of high clinical value. Nikolaos N. Tsiaparas et al [5] proposed a comparative study on multiresolution approach for texture classification of atheromatous plaque from B-mode ultrasound images. They suggested that that wavelet-based texture analysis may be promising for characterizing atheromatous tissue. P. Loizou et al [6] analyzed the walls or layers of the artery for the identification of plaque by using AM-FM features. But this is limited to thin layer and due to the presence of speckle noise the visual and automatic analysis in ultrasound images gets hindered. Jose C. Seabra et al [7] proposed a method for plaque characterization in IVUS data based on a mixture of Rayleigh distributions. The coefficients and parameters of the mixture model are used as features for describing fibrotic, lipidic, and calcified plaques and is classified using AdaBoost classifier. The Rayleigh distribution is widely used to describe homogeneous areas in ultrasound images. Since plaques may contain tissues with heterogeneous regions, distributions depending on multiple parameters are usually needed, such as Rice, K or Nakagami distributions. C. Takanori Koga et al [8] proposed fully automatic and semi-automatic plaque boundary extraction techniques for an intravascular ultrasound (IVUS) image using Fuzzy Inference based method and it involves the future work of automatic adjustment of parameters along with the speed up of each calculation process. Monireh Sheikh Hosseini et al [9] reviewed the application of adaptive neuro-fuzzy inference system as classifier for different medical image classification during the past 16 years.

In this paper, the automatic characterization of atheromatous plaque has been done using the adaptive neuro-fuzzy inference system. To classify each pixel, the input given to the classifier is 16 pixels scanned across the 4×4 window of the corresponding pixel, one output that tells whether the pixel under consideration is Fibrotic, Lipidic, Calcified or Normal pixel.

II. Proposed Methodology

The basic steps involved in proposed methodology are shown in Fig. 1. The various stages include training and testing data formation by pixel intensity from a 4×4 overlapping

D. Selvathi and N. Emimal are with Department of Electronics and Communication Engineering, MEPCO Schlenk Engineering College, Sivakasi, Virudhunagar 626 005, Tamilnadu, India (e-mail: dselvathi@gmail.com).

Henry Selvaraj is with University of Nevada Las Vegas, Las Vegas, USA (e-mail: Henry.Selvaraj@unlv.edu).

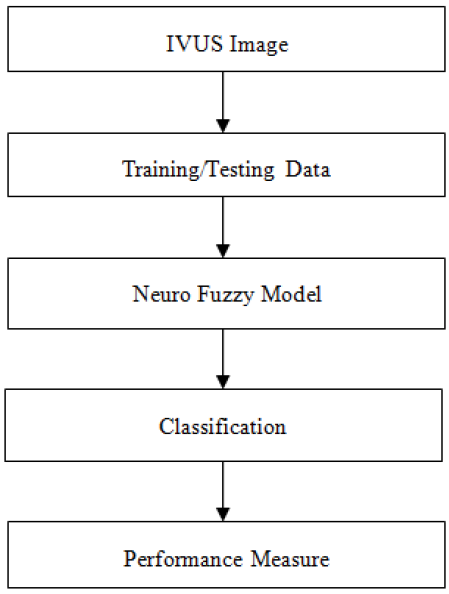

Fig. 1. Proposed methodology.

window, modelling of Neuro Fuzzy system, Classification and Performance Analysis.

III. IVUS Artery Images

Diagnostic imaging is an invaluable tool in medicine today. There are different ways of acquiring artery images such as ultrasound, coronary angiography, cardiac CT and cardiovascular MRI. Among these ultrasound images are most commonly used because they are inexpensive, do not require ionizing radiations and are faster than other radiographic techniques. Also the penetrating nature of IVUS imaging technique helps for the visualization of the blood flow in the artery. Intravascular Ultrasound images used in this work are grayscale images and these are collected from the available resources [7]. The corresponding manually segmented ground truth images are also available.

IV. Training/Testing Data

The Training image is of size 294294 and it consists of fibrotic, lipidic, calcified and normal tissue. The inputs to the Neuro Fuzzy classifier are limited to intensity values from a (4×4) overlapping window scanned across the particular training image for each pixel. The testing image may be affected by the combination of plaque tissues or it can be a normal artery image.

V. Neuro Fuzzy Classifier

A neuro-fuzzy classifier uses a learning algorithm derived from or inspired by neural network theory to determine its parameters (fuzzy sets and fuzzy rules) by processing data samples. The basic steps involved in neuro fuzzy model is Clustering the Data, Generating the Fuzzy Inference System (FIS) and Understanding the Clusters-FIS Relationship.

A. Clustering the Data

In this step, model the relationship between the input variables (16 pixels from a 4×4 overlapping window) and the output variable by first clustering the data. Clustering can be a very effective technique to identify groupings in data from a large data set, thereby allowing concise representation of relationships embedded in the data. The cluster centers will then be used as a basis to define a Fuzzy Inference System (FIS) which can then be used to characterize the atheromatous plaque. K-means algorithm is used to initiate the fuzzy rules. K-means is one of the simplest unsupervised learning algorithms that classify a given data set into certain number of clusters (assume k clusters) fixed a priori [10]. The main idea is to define k centroids, one for each cluster. The K-mean algorithm uses the following distance formula to compute the distance of the n data points from their respective j-th cluster centre.

$$j = \sum_{j=1}^{k} \sum_{i=1}^{x} ||x_i^{(j)} - c_j||^2 \tag{1}$$

where $||x_i^{(j)} - c_j||^2$ is a distance measure between a data point $x_i^{(j)}$ and the cluster centre, c_j.

B. Generating the Fuzzy Inference System (FIS)

FIS is a network-type structure, which maps inputs through input membership functions and associated parameters, and then through output membership functions and associated parameters to outputs, can be used to interpret the input/output map. A type of fuzzy inference such as Sugeno is used in which the consequent of each rule is a linear combination of the inputs. The output is a weighted linear combination of the consequents. It is computationally efficient, works well with linear techniques, optimization and adaptive techniques, has guaranteed continuity of the output surface and it is well suited to mathematical analysis. For simplicity, here a network with two inputs, x and y and one output f is considered in general. A typical rule in a Sugeno fuzzy model has the form:

Rule 1: If x = A_1 and $y = B_1$, then

$$Output\ is\ f_1 = p_1 x + q_1 y + r_1 \tag{2}$$

Rule 2: If x = A_2 and y = B_2, then

$$Output\ is\ f_2 = p_2 x + q_2 y + r_2 \tag{3}$$

where x and y are the inputs. The output level fi of each rule is weighted by the firing strength wi of the rule. p_i, q_i and r_i are the design parameters which are determined using the training process. The computation of these parameters (or their adjustment) is facilitated by a gradient vector, which provides a measure of how well the fuzzy inference system is modeling the input/output data for a given set of parameters. Once the gradient vector is obtained, optimization routines could be applied in order to adjust the parameters so as to reduce some error measure (usually defined by the sum of the squared difference between actual and desired outputs). The

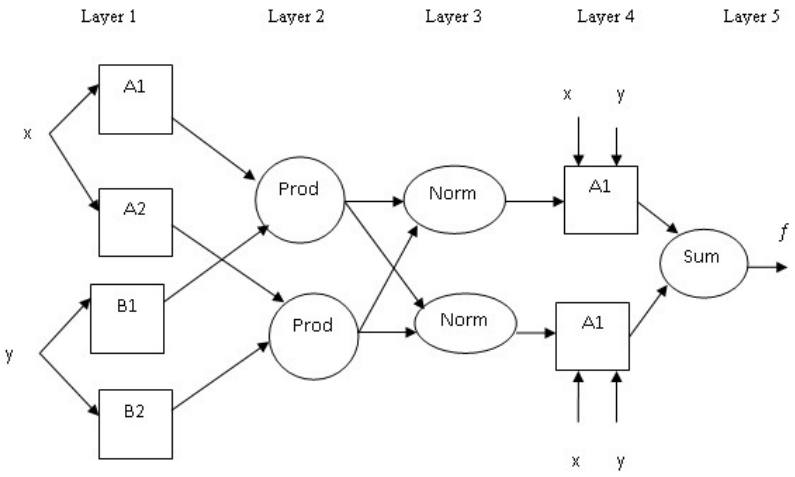

Fig. 2. General ANFIS structure.

ANFIS architecture to implement these two rules is shown in Fig. 2, in which a circle indicates a fixed node whereas a square indicates an adaptive node. As figure illustrates, ANFIS architecture consists of five layers.

The final output of the system is the weighted average of all rule outputs, computed as

$$Final\ Output = \frac{\sum_{i=1}^{N} w_i z_i}{\sum_{i=1}^{N} w_i} \tag{4}$$

where N denotes the number of rules. For plaque characterization, ANFIS structure includes sixteen inputs and one output with four rules. Hence, the Fuzzy inference process comprises of five parts: Fuzzification of the input variables, application of the fuzzy operator (AND or OR) in the antecedent, implication from the antecedent to the consequent, aggregation of the consequents across the rules, and Defuzzification.

C. Understanding the Clusters-FIS Relationship

A FIS is composed of inputs, outputs and rules. Each input and output can have any number of membership functions. The rules dictate the behavior of the fuzzy system based on inputs, outputs and membership functions. Gaussian membership function is only used for fuzzy set descriptions, because of its simple derivative expressions. For plaque characterization, rule base comprises of four rules, which can classify the target pixel.

VI. Performance measure

The classification performance can be evaluated either qualitatively or quantitatively. The qualitative measurement shows only the visual results and it can only be described whereas the quantitative evaluation can provide precise results reflecting the exactness of evaluation. In this work, the quantitative evaluation of the different classification maps is carried out, in the pixel level, via the concept of confusion matrix which is a specific table layout that measures the performance of an algorithm, typically a supervised learning one.

A. Confusion Matrix

In predictive analytics, a table of confusion (also called a confusion matrix), is a table with two rows and two columns that reports the number of false positives, false negatives, true positives, and true negatives. Each column of the matrix represents the instances in a predicted class, while each row represents the instances in an actual class. This allows more detailed analysis than mere proportion of correct guesses (accuracy). Accuracy is not a reliable metric for the real performance of a classifier, because it will yield misleading results if the data set is unbalanced (that is, when the number of samples in different classes vary greatly). The confusion matrix is shown in Tab. I.

TABLE I
Confusion Matrix

Condition (as determined by "Gold Standard")	Test Outcome	
	Positive	Negative
Positive	True Positive (TP)	False Negative (FN)
Negative	False Positive (FP)	True Negative (TN)

B. Sensitivity

Sensitivity is the statistical measure which provides the proportion of actual positives which are correctly identified.

$$Sensitivitiy = \frac{TP}{TP + FN} \tag{5}$$

C. Specificity

Specificity is the statistical measure which provides the proportion of negatives which are correctly identified

$$Specificity = \frac{TN}{TN + FP} \tag{6}$$

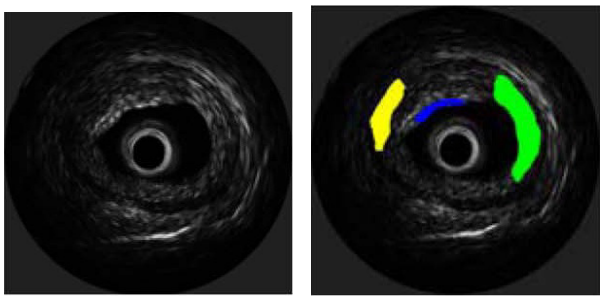

(a) (b)

Fig. 3. (a) Training image, (b) ground truth.

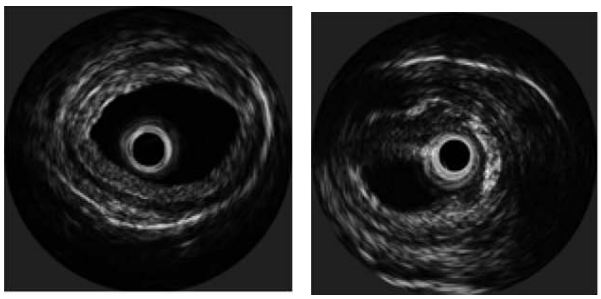

(a) (b)

Fig. 4. Sample Images used in the testing phase.

D. Accuracy

Accuracy reflects the overall correctness of the classifier

$$Accuracy(\%) = \frac{TP + TN}{TP + TN + FP + FN} \cdot 100 \qquad (7)$$

VII. Results and Discussion

In this work, the IVUS image affected by three types of plaque content such as fibrotic, lipidic and calcified is used as the training image. The three types of plaque content are identified through the manually segmented image and hence the corresponding input image is used for training. The training image used and the corresponding manually segmented image are shown in the Fig. 3.

For segmentation based on pixel classification, training and testing data are required. The classifier is trained using the data extracted from the training image and to evaluate the performance of trained classifier, testing images are needed. The sample testing images used in this work are shown in the Fig. 4. The training data includes the intensity values from a (4×4) overlapping window for each pixel scanned across the particular training image. Hence it has sixteen inputs and one output that tells whether the pixel under consideration is Fibrotic, Lipidic, Calcified or Normal pixel. Rule base comprises of four rules, which can classify the target pixel. Thus, using the trained classifier, the plaque affected regions in the untrained images are segmented and it is shown in the Fig. 5. Here, the fibrotic affected samples are represented as green color, lipidic affected by yellow color, calcified affected samples are represented as blue color and the normal pixels are black color as color representation.

The Confusion Matrix of two sample testing images for plaque characterization are shown in the Tab. II and the corresponding quantitative measurements for individual and overall classes are shown in the Tab. III and the Tab. IV respectively.

TABLE II
Confusion Matrix

		Predicted Class				
		F	L	C	N	T
Actual Class	F	996	415	0	0	**1,411**
	L	0	0	0	0	**0**
	C	0	57	2,028	175	**2,260**
	N	0	0	385	82,380	**82,765**
	T	**996**	**472**	**2,413**	**82,555**	**86,436**

(a) For Testing Image 1

		Predicted Class				
		F	L	C	N	T
Actual Class	F	1318	228	0	0	**1546**
	L	0	0	0	0	**0**
	C	0	2	1381	129	**1512**
	N	0	0	210	83,168	**83,378**
	T	**1318**	**230**	**1591**	**83,297**	**86,436**

(b) For Testing Image 2

		Predicted Class				
		F	L	C	N	T
Actual Class	F	0	0	0	0	**0**
	L	204	604	0	746	**1554**
	C	0	0	0	0	**0**
	N	0	0	862	84,02	**84,882**
	T	**204**	**604**	**862**	**84,766**	**86,436**

(c) For Testing Image 3

		Predicted Class				
		F	L	C	N	T
Actual Class	F	2312	623	0	0	**2935**
	L	14	1482	0	66	**1562**
	C	0	0	293	181	**474**
	N	0	0	68	81,397	**81,465**
	T	**2326**	**2105**	**361**	**81,644**	**86,436**

(d) For Testing Image 4

		Predicted Class				
		F	L	C	N	T
Actual Class	F	3415	194	0	0	**3609**
	L	0	0	0	0	**0**
	C	0	0	0	0	0
	N	0	0	160	82,667	**82,827**
	T	**3415**	**194**	**160**	**82,667**	**86,436**

(e) For Testing Image 5

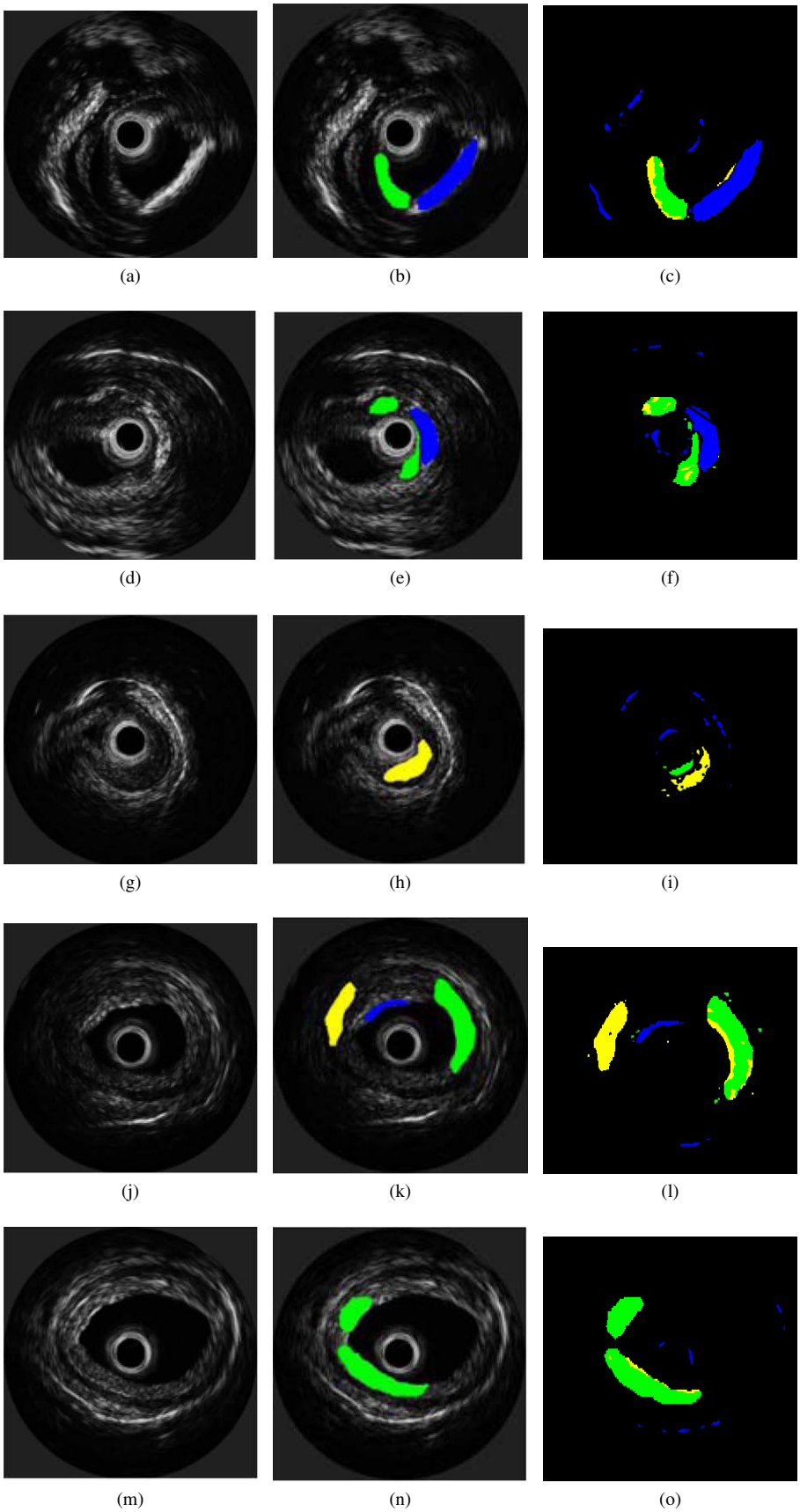

Fig. 5. Segmentation results: (a), (d), (g), (j) & (m) – testing images; (b), (e), (h), (k) & (n) – ground truth images; (c), (f), (i), (l) & (o) – segmented images.

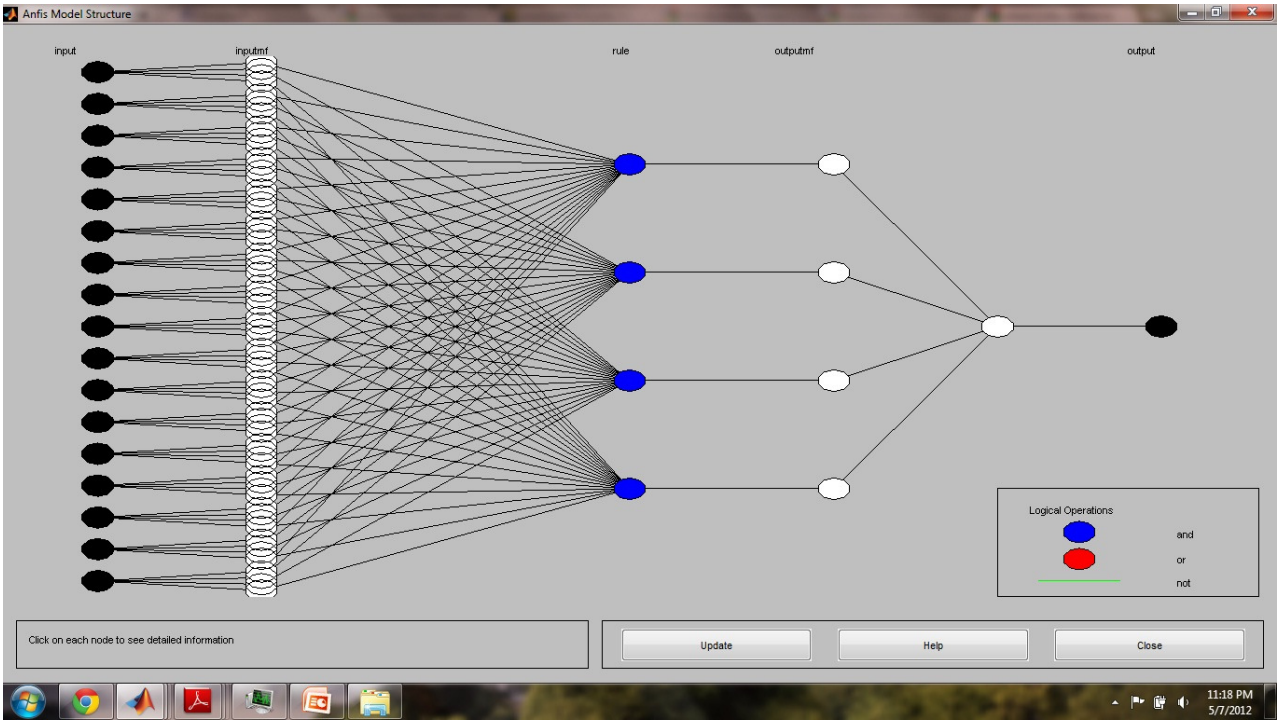

Fig. 6. ANFIS structure for a sample pixel classification.

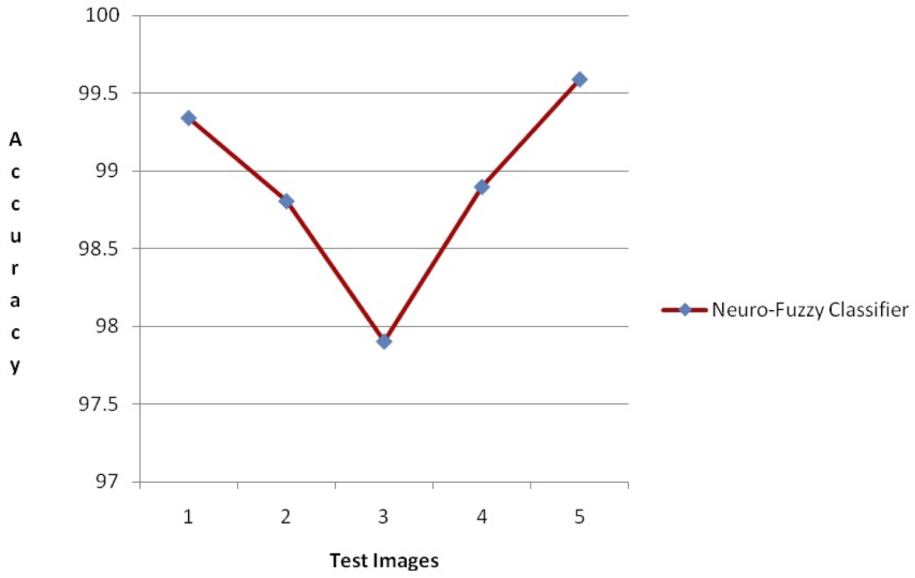

Fig. 7. Accuracy plot.

Figure 6 shows the ANFIS architecture for a sample pixel classification which includes the sixteen inputs plus one bias input concluded by the single output in which it tells the particular pixel belongs to which class.

In Tab. II, for testing image 1, a total of 1,411 pixels are actually affected by fibrotic. Among these, 996 pixels are correctly predicted as the fibrotic tissue and the remaining 415 pixels are wrongly predicted as lipidic tissue. Also the actual class never contains the lipidic content. But the classifier incorrectly predicts the existence of lipidic tissue of about 472 pixels. Then, among 2,260 calcified affected pixels, only 2,028 pixels are predicted correctly as calcified tissue and the remaining 57 pixels are incorrectly predicted as lipidic and 175 pixels as normal. For normal tissue, among 82,765 pixels, only 82,380 pixels are correctly classified as normal tissue and the remaining 385 pixels are incorrectly predicted as the calcified tissue. Similarly Tabs. II(b), II(c), II(d), II(e) shows the details about the classified output for testing image 2, testing image 3, testing image 4 and testing image 5 respectively.

TABLE III
QUANTITATIVE ANALYSIS FOR SEGMENTED RESULTS

	Images	Sensitivity	Specificity	Accuracy
1	Fibrotic	0.8525	1	99.7362
	Lipidic	Undefined	0.9973	99.7339
	Calcified	0.9134	0.9975	99.6055
	Normal	0.9975	0.9316	99.6024
2	Fibrotic	0.7059	1	99.5199
	Lipidic	Undefined	0.9945	99.4539
	Calcified	0.8973	0.9954	99.2862
	Normal	0.9953	0.9112	99.3391
3	Fibrotic	Undefined	0.9976	99.7640
	Lipidic	0.3887	1	98.9009
	Calcified	Undefined	0.9900	99.0027
	Normal	0.9898	0.6912	98.1520
4	Fibrotic	0.7877	0.9998	99.2630
	Lipidic	0.9488	0.9927	99.1867
	Calcified	0.6181	0.9992	99.7119
	Normal	0.9992	0.9480	99.6346
5	Fibrotic	0.9462	1	99.7756
	Lipidic	Undefined	0.9978	99.7756
	Calcified	Undefined	0.9981	99.8149
	Normal	0.9981	1	99.8152

TABLE IV
OVERALL ACCURACY FOR SEGMENTED RESULTS

Images	Accuracy (%)
1.	99.3417
2.	98.8061
3.	97.9037
4.	98.8986
5.	99.5904

TABLE V
CLASSIFICATION ACCURACY FOR EXISTING AND PROPOSED SYSTEM FOR PLAQUE CHARACTERIZATION

Classifier	Accuracy (%)
AdaBoost [7]	92.56
Neuro-Fuzzy [Proposed]	98.9

In Tab. III, for testing images 1, 2, 3 and 5 there is an undefined value for sensitivity. This is because the absence of particular plaque content in the corresponding testing images. The Accuracy plot for the five sample images are tested using the trained neuro-fuzzy classifier is shown in the Fig. 7 which shows that the maximum of 99.5904 is achieved for the testing image consists of only the fibrotic and normal tissues.

Jose C. Seabra et al [7] proposed a technique for plaque characterization in IVUS data based on a mixture of Rayleigh distributions. The coefficients and parameters of the mixture model are used as features for describing fibrotic, lipidic, and calcified plaques. In addition to these features, the texture and spectral features are extracted and it is given as input to AdaBoost for classification. The result obtained for the proposed system such as the Neuro-Fuzzy classifier is compared with the result obtained in [7] which is shown in the Tab. V.

Table V shows that the neuro-fuzzy classifier trained with the spatial intensity yields the better classification accuracy around 98.9% compared with AdaBoost classifier trained using the RMM features joined to the textural and spectral features. The average processing time for the training is 700 secs and for testing the processing time is approximately 300 secs.

VIII. CONCLUSION

In the proposed work, atheromatous plaque characterization such as the fibrotic, lipidic, calcified and normal tissue is done using the neuro-fuzzy classifier. In this work, the neuro fuzzy classifier is trained using the sixteen inputs for each pixel, corresponds to sixteen pixels of instantaneous scanning matrix, one output that tells whether the pixel under consideration is Fibrotic, Lipidic, Calcified or Normal pixel. The results confirmed that the neuro fuzzy classifier has the potential in detecting the respective plaque with the average accuracy of 98.9%. The future work includes the plaque characterization by means of choosing the appropriate training features to improve the accuracy. This developed system helps to win a battle against heart disease and stroke mortality.

REFERENCES

[1] World Health Organization, "Fact sheet No. 317," September 2011, [Online] Available: http://www.who.int/cardiovascular diseases/en.

[2] A. Katouzian, S. Sathyanarayana, B. Baseri, E. E. Konofagou, and S. G. Carlier, "Challenges in Atherosclerotic Plaque Characterization with Intravascular Ultrasound (IVUS): From Data Collection to Classification," *IEEE Transaction on Information Technology in Biomedicine*, vol. 12, no. 3, pp. 315–327, 2008.

[3] E. C. Kyriacou, C. Pattichis, M. Pattichis, C. Loizou, C. Christodoulou, S. K. Kakkos, and A. Nicolaides, "A Review of Noninvasive Ultrasound Image Processing Methods in the Analysis of Carotid Plaque Morphology for the Assessment of Stroke Risk," *IEEE Transaction on Information Technology in Biomedicine*, vol. 14, no. 4, pp. 1027–1037, 2010.

[4] L. S. Athanasiou, P. S. Karvelis, V. D. Tsakanikas, K. A. Stefanou, K. K. Naka, L. K. Michalis, G. A. Rigas, and D. I. Fotiadis, "Atherosclerotic plaque characterization using geometrical features from virtual histology intravascular ultrasound images," in *10th IEEE International Conference on Information Technology and Applications in Biomedicine*, 2010, pp. 1–4.

[5] N. N. Tsiaparas, S. Golemati, I. Andreadis, J. S. Stoitsis, I. Valavanis, and K. S. Nikita, "Comparison of Multiresolution Features for Texture Classification of Carotid Atherosclerosis From B-Mode Ultrasound," *IEEE Transactions On Information Technology in Biomedicine*, vol. 15, no. 1, pp. 130–137, 2011.

[6] C. P. Loizou, V. Murray, M. S. Pattichis, and C. S. Pattichis, "Multiscale Amplitude-Modulation Frequency-Modulation (AMFM) Texture Analysis of Ultrasound Images of the Intima and Media Layers of the Carotid Artery," *IEEE Transactions On Information Technology in Biomedicine*, vol. 15, no. 2, pp. 178–187, 2011.

[7] J. C. Seabra, F. Ciompi, O. Pujol, J. Mauri, P. Radeva, and J. Sanches, "Rayleigh Mixture Model for Plaque Characterization in Intravascular Ultrasound," *IEEE Transactions On Biomedical Engineering*, vol. 58, no. 5, pp. 1314–1323, 2011.

[8] T. Koga, E. Uchino, and N. Suetake, "Automated boundary extraction and visualization system for coronary plaque in IVUS image by using fuzzy inference-based method," *IEEE International Conference on Fuzzy Systems*, pp. 1966–1973, 2011.

[9] M. S. Hosseini and M. Zekri, "A review of medical image classification using Adaptive Neuro-Fuzzy Inference System(ANFIS)," *Journal of Medical Signals and Sensors*, vol. 2, no. 1, pp. 51–62, 2012.

[10] R. Kaur, L. Kaur, and S. Gupta, "Enhanced K-Mean Clustering Algorithm for Liver Image Segmentation to Extract Cyst Region," *IJCA Special Issue on Novel Aspects of Digital Imaging Applications*, pp. 59–66, 2011, DOI: 10.5120/4159-323.